Sains Malaysiana 55(10)(2026): 1639-1652
http://doi.org/10.17576/jsm-2026-5510-04

Plasmon-Assisted Visible Light Photocatalytic Activity of Biosynthesized Ag/TiO_2

(Aktiviti Fotopemangkin Cahaya Nampak Berbantukan Plasmon bagi Ag/TiO_2 Biosintesis)

NAZWA JON[1,2], RIZAFIZAH OTHAMAN[1,3,*], MOHAMAD AZUWA MOHAMED[1,3], NURUL AMNI ABDULLAH[1,2], ROZIDA MOHD KHALID[1,3] & ABDEL-NASSER KAWDE[4]

[1]*Department of Chemical Science and Food Technology, Faculty of Science and Technology, Universiti Kebangsaan Malaysia, 43600 UKM Bangi, Selangor, Malaysia*
[2]*Faculty of Applied Sciences, Universiti Teknologi MARA, Perak Branch, Tapah Campus, 35400 Tapah Road, Perak, Malaysia*
[3]*Polymer Research Center (PORCE), Faculty of Science and Technology, Universiti Kebangsaan Malaysia, 43600 UKM Bangi, Selangor, Malaysia*
[4]*Department of Chemistry, College of Sciences, University of Sharjah, P. O. Box 27272 Sharjah, United Arab Emirates*

Received: 31 May 2026/Accepted: 9 September 2026

*Corresponding author; email: rizafizah@ukm.edu.my

ABSTRACT

Green synthesis involves developing and applying techniques that prioritize the environment by minimizing the utilization of harmful substances and reducing waste production. In this study, Ag/TiO_2 photocatalysts were synthesized via a one-pot biosynthesis approach using *Oroxylum indicum* (OI) leaf extract for enhanced photocatalytic activity under visible light irradiation. The OI leaf extract showed the presence of significant amount of phenolic acid (47.3 mg QE/g dry weight) and flavonoid (44.1 mg QE/g dry weight), potentially serving as the main reducing and capping agent in the synthesis process. Physicochemical characterization confirmed that the Ag nanoparticles were decorated on the TiO_2 surface without lattice alteration, as proved by XRD, FESEM, TEM, and XPS. Furthermore, UV–DRS analysis showed a significant reduction in the band gap energy upon Ag incorporation, with 50-Ag/TiO_2 exhibiting the lowest band gap value of 2.09 eV. This reduction was accompanied by enhanced absorption in the visible-light region, which can be attributed to the surface plasmon resonance (SPR) effect of Ag nanoparticles. The Ag/TiO_2 exhibited significant enhancement in photocatalytic activity towards the removal of ciprofloxacin (CIP), achieving 91% for 50-Ag/TiO_2 under visible light irradiation, attributed to improved charge carrier separation. Scavenger and recyclability tests confirmed the dominant role of $\bullet O_2^-$ and the stability of the photocatalyst. A plausible photocatalytic degradation mechanism was proposed based on the experimental findings. This work demonstrates a sustainable strategy for developing plasmonic photocatalysts with enhanced visible light photocatalytic activity for the removal of emerging pollutants.

Keywords: Ag/TiO_2; biosynthesis; ciprofloxacin; photocatalyst; surface plasmon resonance

ABSTRAK

Sintesis hijau melibatkan pembangunan dan penggunaan teknik yang mengutamakan kelestarian alam sekitar dengan meminimumkan penggunaan bahan berbahaya serta mengurangkan penghasilan sisa. Dalam kajian ini, fotomangkin Ag/TiO_2 disintesis melalui pendekatan biosintesis satu langkah menggunakan ekstrak daun *Oroxylum indicum* (OI) bagi meningkatkan aktiviti fotomangkin di bawah sinaran cahaya nampak. Ekstrak daun OI menunjukkan kehadiran sejumlah besar asid fenol (47.3 mg QE/g berat kering) dan flavonoid (44.1 mg QE/g berat kering), yang berpotensi bertindak sebagai agen penurun dan penstabil utama dalam proses sintesis. Pencirian fizikokimia mengesahkan bahawa nanopartikel Ag terdekorasi pada permukaan TiO_2 tanpa perubahan pada struktur kekisi, seperti yang dibuktikan melalui analisis XRD, FESEM, TEM dan XPS. Selain itu, analisis UV-DRS menunjukkan bahawa penggabungan Ag telah menyebabkan pengurangan yang ketara dalam tenaga jurang jalur dengan 50-Ag/TiO_2 mencatatkan nilai jurang jalur terendah iaitu 2.09 eV. Pengurangan ini disertai oleh peningkatan penyerapan dalam kawasan cahaya nampak, yang boleh dikaitkan dengan kesan resonans plasmon permukaan (SPR) nanozarah Ag. Ag/TiO_2 menunjukkan peningkatan ketara dalam aktiviti fotomangkin terhadap penyingkiran ciprofloksacin (CIP) sebanyak 91% bagi 50-Ag/TiO_2 di bawah cahaya nampak, yang dikaitkan dengan pemisahan pembawa cas yang cekap. Ujian pemerangkap radikal dan kebolehgunaan semula mengesahkan peranan dominan radikal $\bullet O_2^-$ serta kestabilan fotomangkin tersebut.

Mekanisme degradasi fotomangkin yang munasabah telah dicadangkan berdasarkan keputusan uji kaji. Kajian ini menunjukkan satu strategi mampan dalam pembangunan fotomangkin plasmonik dengan aktiviti fotomangkin cahaya nampak yang dipertingkatkan untuk penyingkiran bahan pencemar.

Kata kunci: Ag/TiO_2; biosintesis; ciprofloksacin; degradasi antibiotik; fotomangkin; resonans plasmon permukaan

INTRODUCTION

Photocatalysis is an emerging approach for treating various types of wastewaters. This technique is gaining considerable attention for being environmentally friendly, highly efficient, and able to degrade pollutants into less harmful products (Nasrollahzadeh & Mohammad Sajadi 2016). Among the most used photocatalysts is Titanium dioxide (TiO_2), which has various practical applications, including water treatment, solar cells, biomedicine, and cosmetics. The unique properties of TiO_2, such as low cost, non-toxic, readily available, and excellent chemical and photostability, have contributed to its widespread application in wastewater treatment (Azami et al. 2017; Kanakaraju et al. 2022; Mezni 2020). TiO_2 photocatalysts are most effective when exposed to ultraviolet (UV) light because of their huge bandgap energy (3.0-3.2 eV). The UV region makes up about 5% of the total solar light spectrum, which limits its use in practical applications (Khan & Shah 2023). Moreover, the photocatalytic performance of TiO_2 is limited by the rapid recombination of electron and hole pairs. Modifications through doping TiO_2 with other metals (Pb, Zn, Fe), metal oxides (ZnO, Fe_3O_2, CuO), or non-metals (S, N, O, B, F), dye sensitization, and plasmonic metal deposition (Ag, Au, Cu) enhance the photocatalytic performance and broaden the light absorptions into the visible spectrum (Sun et al. 2024; Yin et al. 2017).

Plasmonic metal, such as silver (Ag), is commonly employed as a dopant in numerous applications due to its exceptional electrical conductivity, optical properties, chemical stability, and thermal stability (Singh et al. 2019). In addition, the presence of Ag induces surface plasmon resonance (SPR), resulting in improved visible light absorption. As a result, interfacial charge transfer in TiO_2 will be more efficient. Previous studies reported that depositing TiO_2 with Ag enhanced the photocatalytic activities for the degradation of recalcitrant pollutants (Kanakaraju et al. 2022; Nguyen 2020; Rajangam et al. 2020; Sambaza, Maity & Pillay 2019). Considering these remarkable improvements, the development of straightforward and economical methods for synthesizing Ag/TiO_2 photocatalysts is vital. Various methods can be employed to synthesize Ag/TiO_2, including thermal decomposition, vapor deposition, solvothermal synthesis, laser ablation, and chemical reduction of metal ions. However, the use of costly reagents, slow, tedious processes, high energy consumption, and environmental toxicity are significant concerns with these methods (Cantarella et al. 2023; Kulal & Shetty Kodialbail 2021). In contrast, biosynthesis of nanoparticles is an environmentally benign and economical technique that utilizes plant extract to synthesize metal and metal oxide nanoparticles (Amutha et al. 2023; Raduwan et al. 2022). Various studies employed plant extracts, such as *Cleistocalyx operculatus* leaf (Nguyen 2020), *Thevetia peruviana* fruit (Chelli, Chakraborty & Golder 2018), *Ocimum tenuiflorum* leaf (Saha, Kumar & Sengupta 2019), and *Beta vulgaris* peel (Jayapriya & Arulmozhi 2021) to synthesize Ag/TiO_2.

The phytochemical compounds in plant extract include polyphenols, tannins, flavonoids, terpenoids, alkaloids, glycosides, and saponins (Karim et al. 2019; Moghni et al. 2025; Saif et al. 2023). These compounds function as capping agents that inhibit nanoparticle aggregation and enhance stability, while also acting as reducing agents that lower the valence state of metal ions. The stability of the nanoparticle is achieved through steric hindrance, which is initiated by the interactions between the nanoparticle surface and the phytochemicals present within the plant extract (Selvanathan et al. 2021). *Oroxylum indicum* (OI) is a medicinal plant rich in antioxidants and traditionally used to treat fever, tonsils, asthma, and jaundice (SatyaEswari et al. 2018). OI is typically cultivated in countries with tropical and subtropical climates, such as Southeast Asia (Jagetia 2021). OI is reported to contain abundant metabolites, including polyphenols such as phenolic acids, flavonoids, alkaloids, and tannins in different plant parts, including bark, leaves, flowers, stalks, and seeds (Rojsanga, Bunsupa & Sithisarn 2020).

Biosynthesis using plant extracts has emerged as a sustainable and environmentally friendly alternative for the preparation of metal and metal oxide nanomaterials. Despite the growing interest in green synthesis routes, the influence of phytochemical-mediated synthesis on the formation of plasmonic metal-semiconductor interfaces and their corresponding photocatalytic properties remains insufficiently understood. Therefore, this study investigates the phytochemical-mediated synthesis of Ag/TiO_2 using OI leaf extract and examines how the resulting nanostructure influences photocatalytic performance under visible light irradiation. The successful incorporation of Ag on the TiO_2 surface and its impact on visible light absorption were confirmed through structural, optical, and surface characterizations. The photocatalytic activity was evaluated using ciprofloxacin (CIP) as a representative pollutant, with a radical scavenger test conducted to identify the dominant reactive species. This interfacial configuration induces SPR, suppresses charge carrier recombination, and

significantly enhances the photocatalytic performance of Ag/TiO_2 towards CIP removal under visible light. In addition, a plausible photocatalytic mechanism derived from experimental results is proposed to elucidate the role of Ag in improving visible light activity.

MATERIALS AND METHODS

MATERIALS

Fresh OI leaves were obtained from Baling, Kedah, Malaysia. Silver nitrate, $AgNO_3$ (99.9%), was supplied by POCH S.A., while Titanium (IV) isopropoxide, TTIP (97%), was supplied by Sigma-Aldrich, and ciprofloxacin was supplied by Chemcruz. Sodium chloride (NaCl) and sodium carbonate (Na_2CO_3) were supplied by LOBA Chemie. Quercetin dihydrate, gallic acid, and Follin-Ciocalteu reagent were supplied by SRL, aluminum chloride ($AlCl_3$) was supplied by Bendosen, and sodium acetate ($C_2H_3NaO_2$) was supplied by R&M Chemicals.

SYNTHESIS OF Ag/TiO_2 NANOPARTICLES

The synthesis method was adapted from the procedure reported by Rao et al. (2019) with several modifications. OI leaves were washed, air-dried, and ground to obtain powder form. The powdered leaves were weighed and mixed with distilled water in a 1:20 ratio, then heated at 60 ºC for 30 min. Then, the crude extract was filtered. To synthesize Ag/TiO_2, 5 mL of OI extract was added to 45 mL of $AgNO_3$ solution with concentrations of 10, 30, 50, and 80 mM, and stirred for 60 min at room temperature. The prepared samples were denoted as 10-Ag/TiO_2, 30-Ag/TiO_2, 50-Ag/TiO_2, and 80-Ag/TiO_2. Then, 1.5 mL of TTIP was added, and stirred for 24 h. The formed precipitate was centrifuged and repeatedly rinsed with water. After being dried overnight, the precipitate was calcined for 2 h at 500 ºC.

PHYTOCHEMICAL ANALYSIS OF *Oroxylum indicum* EXTRACT

Total Flavonoid Content (TFC)

The determination of TFC was conducted using the $AlCl_3$ colorimetric method, which was adopted from Chandra et al. (2014) including certain adjustments. An aliquot of 1 mL of extract or quercetin standard solution (5, 100, 250, and 500 µg/mL) was added with 3 mL of methanol, 200 µL of 10% $AlCl_3$, 200 µL of 1M $C_2H_3NaO_2$, and 5.6 mL of distilled water. The absorbance of both the standards and the sample was measured at 420 nm. The results were given in mg quercetin (QE)/g of dried plant material.

Total Phenolic Content (TPC)

The TPC measurement was conducted via the Follin-Ciocalteu phenol reagent (Chandra et al. 2014) with some modifications. An aliquot of 1 mL of the extracts or gallic acid standard solution, with a concentration ranging from 100 to 500 µg/mL, was added to 0.2 mL of Follin Ciocalteu reagent, 0.6 mL of 7.5% Na_2CO_3, and 3.2 mL of distilled water. The mixtures were incubated at room temperature for 2 h. The absorption spectrum of the reaction mixture was scanned in the range of 400-800 nm, and the maximum absorbance (λ_{max}) was observed at 765 nm. Therefore, all measurements were performed at this wavelength. The results were given in mg gallic acid (GAE)/g of dried plant material.

Characterization of Ag/TiO_2 nanoparticles

The diffraction pattern of the nanoparticles was identified using an XRD (Bruker-D8 Advance) with Cu Kα radiation (1.54059 Å). The Scherrer formula, as given in Equation (1), was applied to calculate the crystallite size.

$$D = \frac{K\lambda}{\beta \cos \theta} \quad (1)$$

where K (0.154 nm) represents the X-ray wavelength; β is the FWHM (radians); and θ is the diffraction angle. The morphology was characterized using FESEM (ZEISS SUPRA 55VP) and HRTEM (TALOS L120C). Energy-dispersive X-ray spectroscopy (EDS) was employed for elemental analysis. XPS measurements using a Kratos Axis Ultra DLD spectrometer were performed by employing a monochromatic Al source. All binding energies were calibrated using the C 1s peak (284.85 eV) as the reference. The optical properties and bandgap were investigated using a UV-DRS (UV-VIS, Perkin Elmer Lambda 950). The bandgap of the nanoparticles was measured using the Kubelka-Munk function as in Equation (2).

$$F(R) = \frac{(1-R)^{1/2}}{2R} = \frac{k}{s} \quad (2)$$

where R denotes absolute reflectance; k is the molar absorption coefficient; and s is the scattering coefficient. The PL spectra were obtained using a PL spectrophotometer (Edinburgh Instrument, FLS920).

Photocatalytic activity

The photocatalytic activity of the photocatalyst was performed based on the method described by Suwannaruang et al. (2020), with modifications. The photocatalytic experiments were conducted under visible light irradiation using a 150 W UFO LED lamp (6000 K, 220 V), which emits a broad spectrum within the visible light region (approximately 400-700 nm). The experiment was carried out by adding 75 mg of Ag/TiO_2 to 50 mL of 10 ppm CIP under constant stirring. Prior to LED irradiation, the suspension was stirred in the dark for 60 min until the adsorption-desorption equilibrium was reached. The reactions were conducted

for 240 min to determine the photocatalytic, adsorption, and photolysis processes. Every 30 min, 2 mL aliquots were collected and filtered using 0.45 μm Teflon filter disk to separate the photocatalyst. Absorbance spectra were obtained using UV-visible spectroscopy (Shimadzu UV-1650 PC). The absorption spectra of all samples were recorded in the wavelength range of 200-400 nm. The CIP concentration was determined at 273 nm, corresponding to the characteristic maximum absorption wavelength (λ_{max}) of CIP reported by Li, Liu and Li (2018) and Suwannaruang et al. (2020). The removal percentage of CIP was determined using Equation (3):

$$Removal\ (\%) = \frac{C_0 - C_t}{C_0} = \times\ 100\% \qquad (3)$$

where C_0 is a CIP initial concentration; and C_t is a CIP concentration measured at the instantaneous time.

RESULTS AND DISCUSSION

PHYTOCHEMICAL ANALYSIS OF OI EXTRACT AND MECHANISM OF Ag/TiO_2 FORMATION

The result for TPC in the OI leaves extract was determined from the calibration curve ($y = 0.0015x + 0.0073$; $R^2 = 0.996$, where the result was expressed in gallic acid equivalence (GAE) per gram of dried plant. The TPC of OI leaf extract was found to be 47.3 mg GAE/g. Meanwhile, the result for TFC in the OI leaves extract was measured using the calibration curve equation of $y = 0.0042x + 0.0137$; $R^2 = 0.993$, in which the result was expressed in quercetin equivalence (QE) per gram of dried plant. The TFC of OI leave extract was 44.1 mg QE/g. The present study demonstrated that the TPC and TFC results in aqueous OI leaves extract were relatively high compared to other plant extracts, as shown in Table 1. Flavonoids and other phenolic compounds are typically recognized as secondary metabolites, including an aromatic ring with at least one hydroxyl group (Tungmunnithum et al. 2018). During the synthesis reaction, the hydroxyl group (-OH) and ketone group(-C=O) bind to Ag^+ and reduce to form Ag nanoparticles. It has been reported that all of the hydrophilic polyphenolic compounds obtained from the leaf extract include at least two -OH groups, making them potential participants in a redox process (Aslam, Abdullah & Rafatullah 2021; Rohani et al. 2022). A study by Laouini et al. (2021) proved that the carboxyl, carbonyls, amides, and phenols present in the *Phoenix dactylifera* L. aqueous extract served as reducing and capping agents for Ag/Ag_2O synthesis.

PHYSICOCHEMICAL ANALYSIS

Figure 1 shows the crystallinity and phase of Ag/TiO_2 with different Ag concentrations, as compared to pristine TiO_2. The diffraction peaks of TiO_2 were present in all samples. The diffraction peaks appeared at 25.40º, 37.70º, 48.02º, 53.82º, 44.16º, and 62.70º, associated with the crystal planes of (101), (004), (200), (105), (211), and (204), respectively. The peaks indicate the anatase phase in the formation of TiO_2 nanoparticles (JCPDS file no. 00-021-1272) (Yan, Wu & Liu 2021). Usually, TiO_2 acts effectively as a photocatalyst in the anatase phase (Lee et al. 2017). From the Ag/TiO_2 XRD pattern, no prominent peaks of Ag were seen. Ag peaks usually appear at 38.11º (111), 44.30º (200), and 64.44º (220) according to JCPDS no. 01-087-0597, which may overlap with some TiO_2 anatase peaks (Rahmawati et al. 2023; Rostas et al. 2025). This finding also demonstrates that the size of Ag was relatively small and evenly distributed throughout the TiO_2 crystal structure (Yildirim 2021). The intensity of the TiO_2 (101) major anatase peak decreased and broadened, as can be observed in Figure 1. The decrease in peak intensity was proportional to the amount of Ag added. However, there was no significant shift in the peak position. Table 2 depicts the TiO_2 and Ag/TiO_2 crystallite size of the main TiO_2 (101) peak, where a slight decrease in crystallite size was observed, but there were no significant changes in the TiO_2 crystallite size. The absence of a significant shift in the peak position or crystallite size suggests that Ag was not incorporated into the TiO_2 lattice through substitutional or interstitial doping. This minimal change indicates that the deposition of Ag nanoparticles does not significantly alter the TiO_2 crystal structure or influence the crystallization process of TiO_2. The result

TABLE 1. Comparison of TPC and TFC content in different plant extracts

Extract	TPC (mg GAE/g dry weight)	TFC (mg QE/g dried weight)	Reference
Musa paradisiaca leaves	1.32	0.164	(Rao et al. 2019)
Carica papaya leaves	9.97	2.63	(Cosmas Mojulat & Surugau 2018)
Severinia buxifolia	5.95	0.63	(Truong et al. 2019)
Oroxylum indicum leaves	47.3	44.1	This study

suggests that Ag nanoparticles are mainly deposited on the surface of TiO_2 rather than incorporated into the TiO_2 lattice. Notably, the Ag addition did not alter the TiO_2 crystallite size, showing that the insertion of Ag only altered the crystal lattice on the surface of TiO_2. Therefore, it has no effect on the overall TiO_2 bulk structure (Tseng & Chen 2020). Furthermore, Ag^+ ions cannot substitutionally replace Ti^{4+} ions due to the difference in radius of Ag^+ (0.126 nm), which is greater than that of Ti^{4+} (0.068 nm) (Wang et al. 2020).

The presence of Ag on TiO_2 was further studied through morphological analyses. Figure 2(a) and 2(b) shows the FESEM images of TiO_2 and 50-Ag/TiO_2, respectively. As shown in Figure 2(b), the incorporation of biosynthesized Ag does not result in significant changes to the fundamental morphology of TiO_2. The granular, porous network structure is preserved in Ag/TiO_2, suggesting that the Ag deposition does not damage or collapse the porous TiO_2 framework. In addition, the FESEM images reveal the presence of particle agglomeration in both TiO_2, and Ag/TiO_2, where primary particles coalesce to form aggregates. This phenomenon is commonly observed in nanomaterials subjected to high-temperature thermal treatment (Amarjargal, Tijing & Kim 2012; Habibi & Nasr-Esfahani 2008). In this study, particle coalescence likely occurred during the calcination process at 500 ºC, which promotes crystal growth. However, the Ag/TiO_2 sample exhibits a more interconnected network structure compared to TiO_2. This may be attributed to the presence of Ag nanoparticles, which facilitate the formation of interparticle connections between adjacent TiO_2 particles, leading to a more interconnected network structure (Amarjargal, Tijing & Kim 2012). Figure 2(c) and 2(d) shows the elemental compositions of TiO_2 and 50-Ag/TiO_2, respectively. Only two elements were present in TiO_2, which were Ti, 56.4%, and O, 43.6% (total of 100%). In contrast, 14.4% Ag was detected in the Ag/TiO_2. This result clearly confirms that only Ag is present on the TiO_2 surface, suggesting the absence of any other impurities in the sample.

TEM was utilized further to examine the particle structure, size, and phase. Figure 2(e) and 2(f) shows the TEM images of TiO_2 and 50-Ag/TiO_2, respectively. Figure 2(e) showed quasi-spherical particles with some agglomerations, as also indicated in the FESEM image. In Figure 2(f), Ag nanoparticles were spherical, scattered, and deposited on the TiO_2 surface. Ag appeared to be darker than TiO_2 due to a significant density difference between Ag (10.43 g/cm^3) and anatase TiO_2 (3.78 g/cm^3)

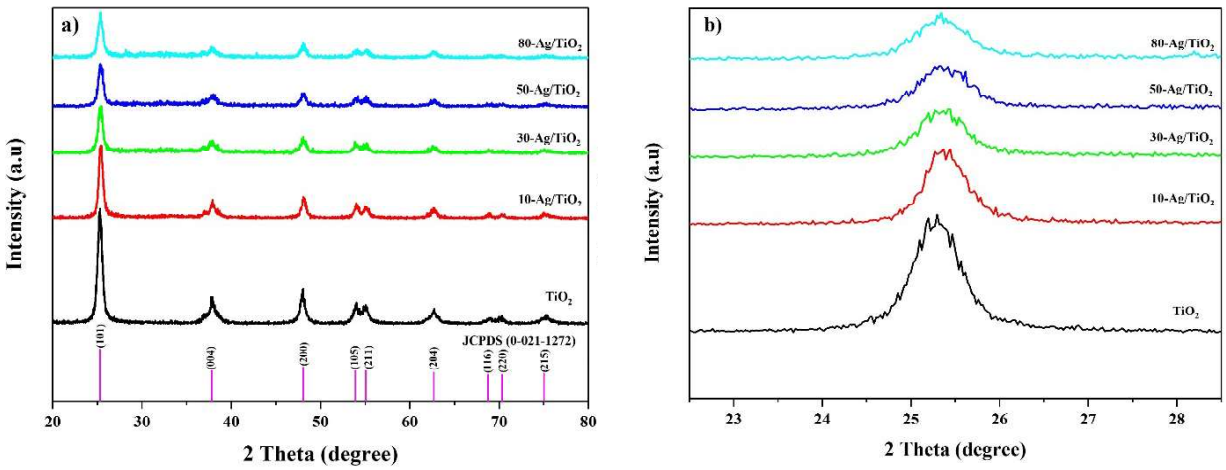


FIGURE 1. XRD pattern of TiO_2 and Ag/TiO_2 samples and (b) intensity of (101) peak

TABLE 2. Crystallite size and bandgap of TiO_2 and Ag/TiO_2 samples

Sample	Anatase crystallite size (101) (nm)	Band gap, E_g (eV)
TiO_2	11.94	3.22
10-Ag/TiO_2	11.82	2.55
30-Ag/TiO_2	11.91	2.24
50-Ag/TiO_2	11.40	2.09
80-Ag/TiO_2	11.15	2.26

(Alkan et al. 2017). Figure 2(g) displays the Ag/TiO_2 high-resolution TEM (HRTEM) image, where the (101) plane of anatase TiO_2 was determined to correspond to the measured lattice spacing of 0.35 nm fringes. In comparison, the (111) of the face-centered cubic (FCC) Ag crystal has a lattice fringe spacing of around 0.23 nm (Paramesh et al. 2021). The finding aligns with the XRD results, which confirmed the presence of anatase TiO_2. Although the distinguished peak of Ag cannot be observed in XRD, the results obtained from TEM and EDX analysis have verified the deposition of Ag on TiO_2. Figure 2(h) shows the particle size distribution of Ag lies between 4 and 12 nm, with the highest distribution at 7-8 nm.

XPS analysis was performed to investigate the chemical states of the nanoparticles. Figure 3(a) shows the high-resolution XPS spectrum of C 1s for both TiO_2 and Ag/TiO_2. The result shows several carbon-related peaks corresponding to C-C, C-O, and C=O functional groups. The spectrum was deconvoluted into three peaks for both TiO_2 and Ag/TiO_2. The C-C peak seen at 284.85 eV in all samples is believed to come from the adventitious carbon species found in the air-exposed and from the extract (Ahmed Sharwani et al. 2021). There were also oxygen-bound C-O found at around 286.85 eV and 286.17 eV for TiO_2 and Ag/TiO_2, respectively. The C=O peaks appear at around 288.33 eV for TiO_2 and 288.94 eV for Ag/TiO_2. The presence of these peaks were attributed to phytochemicals including phenolic acids and flavonoids, which are involved in the reduction and stabilization of the synthesized nanoparticles (Ahmed Sharwani et al. 2021; Nagaraj et al. 2023; Rathi, Jeice & Jayakumar 2023).

Figure 3(b) describes the high-resolution spectra for O 1s of TiO_2 and Ag/TiO_2. Three peaks were observed at 529.52 eV for TiO_2 and 530.08 eV for Ag/TiO_2, related to Ti-O-Ti (Davari et al. 2025; Gao et al. 2019). The shifting of the peak is most likely due to the strong interfacial interaction between Ag nanoparticles and the TiO_2 (Abbas, Rasuli & Nakhostin Panahi 2025; Davari et al. 2025). This interaction promotes charge redistribution at the Ag/TiO_2 interface, leading to upward band bending in TiO_2 and the subsequent formation of a Schottky barrier. Another peak centered at 531.03 eV related to attributed to the presence of OH groups on the TiO_2 (Ratshiedana et al. 2024), and at 532.15 eV related to adsorbed O_2 for both TiO_2 and Ag/TiO_2, respectively (Hariharan et al. 2020). It is essential to notice that the Ti-O-Ti of Ag/TiO_2 has a higher binding energy compared to TiO_2.

The high-resolution spectra of Ti 2p for TiO_2 and Ag/TiO_2 are shown in Figure 3(c) as the peak can be deconvoluted into two peaks attributed to Ti $2p_{3/2}$ and Ti $2p_{1/2}$. The Ti $2p_{3/2}$ and $2p_{1/2}$ binding energies are found to be approximately 458.35 eV and 464.13 eV, respectively, for TiO_2 and 458.86 eV and 464.57 eV, respectively, for Ag/TiO_2. The spin-orbital splitting of binding energy between $2p_{3/2}$ and Ti $2p_{1/2}$ in both samples was around 5.7 eV, in accordance with the chemical state of Ti^{4+} in the anatase TiO_2 (Seo et al. 2023). This finding aligns with the XRD result that showed the presence of anatase.

The presence of Ag was further confirmed in the high-resolution spectra of Ag/TiO_2, as presented in Figure 3(d). The presence of silver in the Ag^0 state is confirmed by the distinct peaks observed at 369.45 eV and 374.92 eV for Ag $3d_{5/2}$ and Ag $3d_{3/2}$, respectively. The binding energies of these values are consistent with the stated values for Ag^0 in the previous reports (Kaur Aulakh et al. 2020; Rahmawati et al. 2023). The Ag^0 generated through the biosynthesis process were successfully reduced to metallic Ag^0.

Figure 4(a) shows the Kubelka-Munk optical absorption for TiO_2 and Ag/TiO_2 nanoparticles. It can be seen that TiO_2 exhibited higher absorption in the 200-400 nm (UV region) as compared to Ag/TiO_2. Upon the deposition of Ag caused a significant shift in the optical reflection edge of pristine TiO_2 from UV to the visible wavelength range (>400 nm) The absorption intensity gradually increased with increasing Ag loading. This is due to the SPR offered by Ag, which causes the reflectance to be red-shifted (bathochromic effect) (Jasrotia et al. 2020). Figure 4(b) depicts the optical bandgap energy that was calculated using the Kubelka-Munk function (Equation 2). The optical bandgap values of TiO_2 and Ag/TiO_2 are presented in Table 2. Pristine TiO_2 exhibited a band-gap energy of 3.22 eV, which is consistent with the typical value reported for anatase TiO_2 (Bhardwaj & Singh 2021; Shi et al. 2019; Zarzzeka et al. 2024). Upon Ag deposition, the optical band-gap value decreased significantly to 2.55, 2.24, 2.09, and 2.20 eV for the 10 mM, 30 mM, 50 mM, and 80 mM Ag/TiO_2, respectively. The narrowed bandgap indicates that less energy is required to excite electrons from the valence band to the conduction band (Abbas, Rasuli & Nakhostin Panahi 2025). This suggests that the presence of Ag enhanced light absorption in the visible region and promotes the generation of photoinduced charge carriers.

The charge separation efficiency of the photocatalysts can be clarified by examining the charge carrier separation of the photocatalysts. Photoluminescence (PL) was employed to further understand the photoexcited charge carrier recombination. The PL emission spectra of TiO_2 and Ag/TiO_2 samples are described in Figure 4(c). The TiO_2 exhibit an intense emission band compared to Ag/TiO_2, showing faster electron and hole recombination. The emission intensity of Ag/TiO_2 samples decreased with 50-Ag/TiO_2 showed the lowest PL intensity among all samples, which indicates lower electron and hole recombination rates (Seo et al. 2023). As discussed in the XPS analysis, the shifts in the Ti 2p and O 1s binding energies suggest a strong electronic interaction at the Ag/TiO_2 interface. Ag nanoparticles deposited on the TiO_2 surface can form a Schottky junction due to their higher work function than TiO_2 (Sabir, Sherazi & Xu 2021). The deposited Ag nanoparticles act as electron

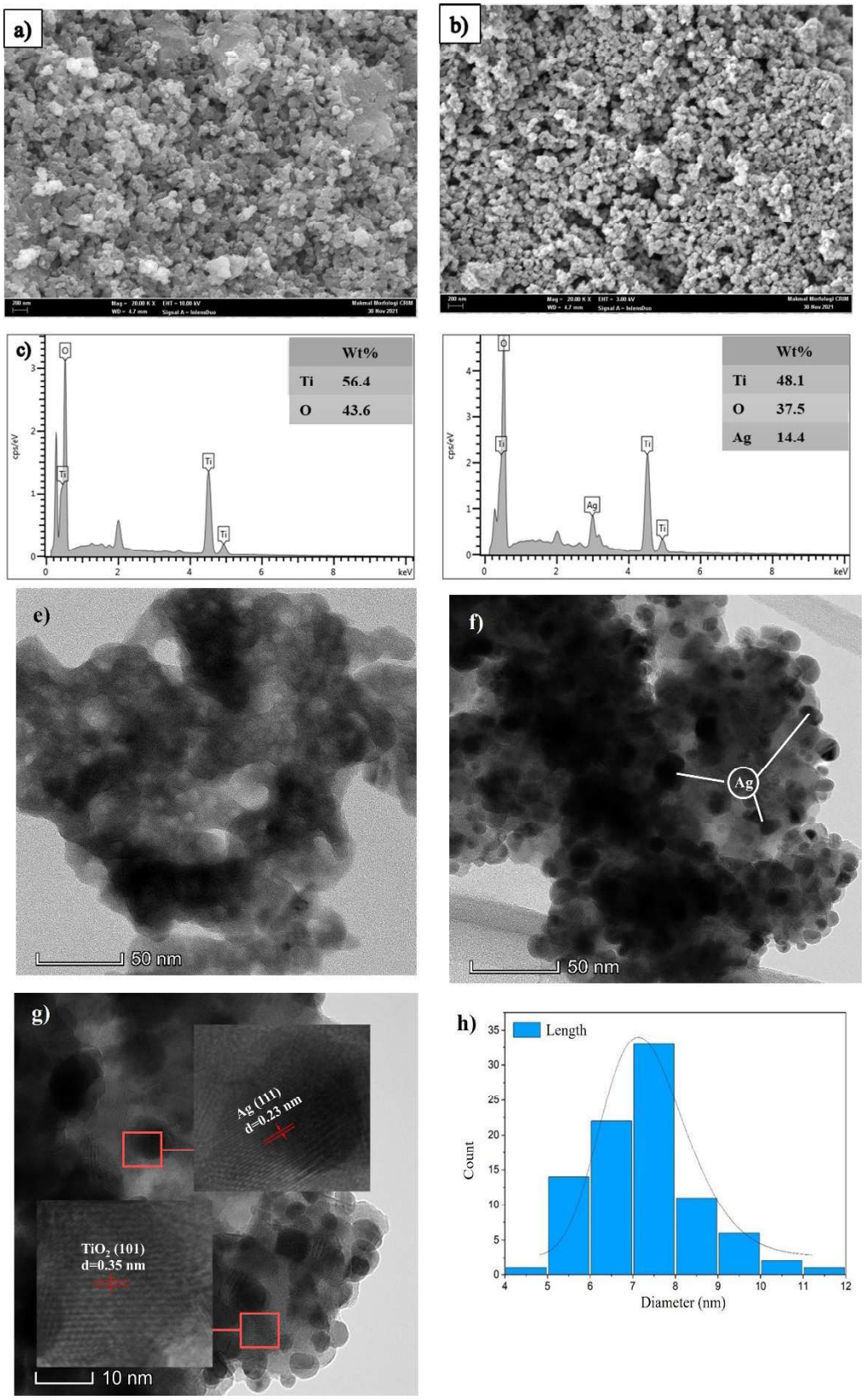


FIGURE 2. (a-b) FESEM images of TiO_2 and Ag/TiO_2 at a magnification of 20000× and (c-d) the corresponding EDX analysis, TEM image of (e) pristine TiO_2 and (f) Ag/TiO_2 (g) HRTEM image of Ag/TiO_2 (h) particle size distribution of Ag decorated on the TiO_2 surface

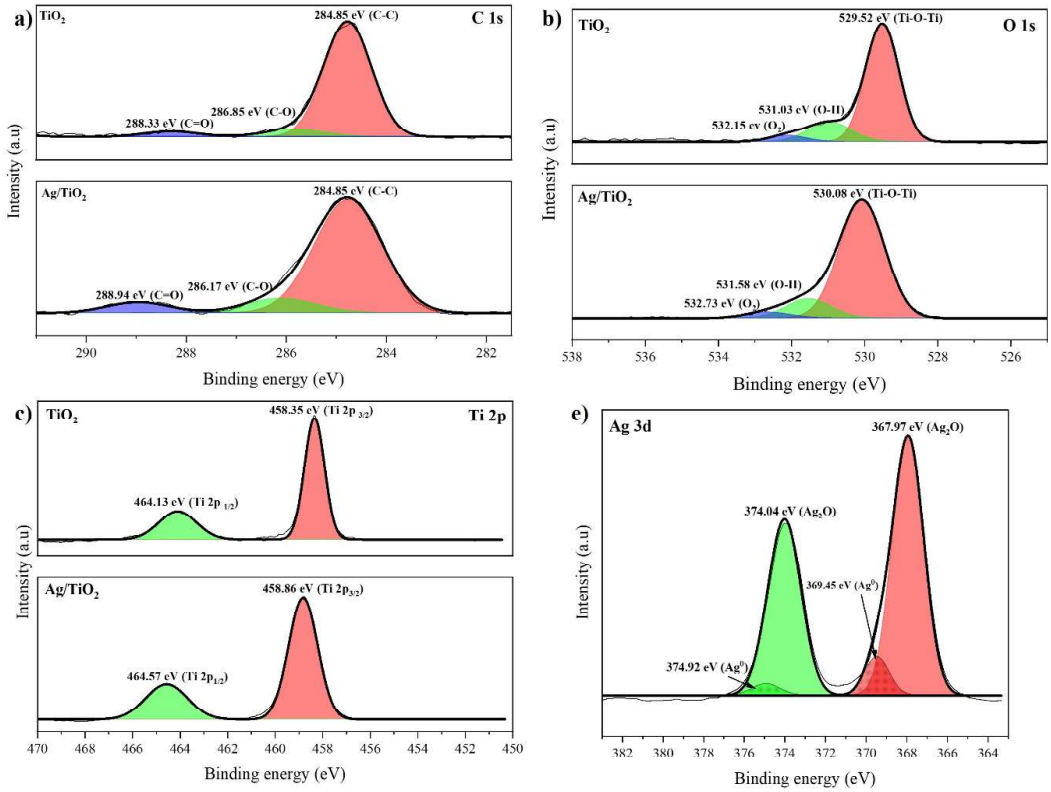


FIGURE 3. High-resolution XPS spectra of (a) C 1s, (b) O 1s, (c) Ti 2p, and (d) Ag 3d of the samples

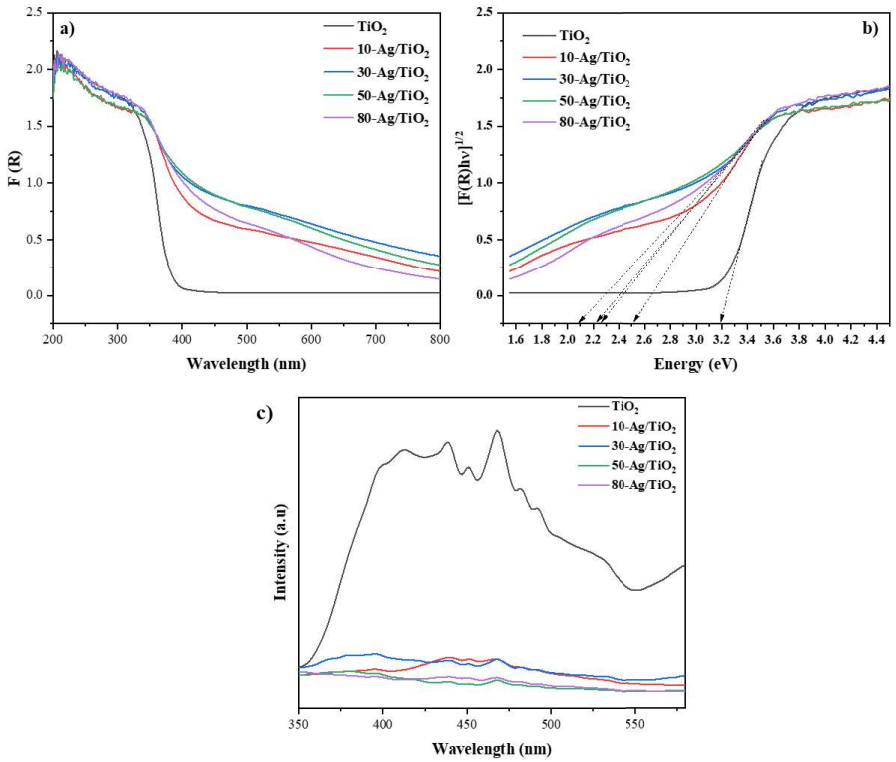


FIGURE 4. Kubelka-Munk optical absorption and (b) Kubelka-Munk plot for the estimation of the bandgap energies of TiO_2 and Ag/TiO_2 samples, and c) PL emission spectra of TiO_2 and Ag/TiO_2 samples

traps, capturing electrons from TiO_2 and thus facilitating electron and hole separation, thereby improving charge separation and reducing electron and hole recombination (Tang et al. 2019; Zarzzeka et al. 2024). The incorporation of Ag not only enhances light harvesting through the SPR effect but also improves charge separation by promoting electron transfer from TiO_2 to Ag nanoparticles, thereby suppressing electron and hole recombination.

PHOTOCATALYTIC ACTIVITY

Figure 5 describes the photocatalytic activity of TiO_2 and Ag/TiO_2 nanoparticles for the CIP removal under visible light irradiation. The absorbance of CIP was observed at λ_{max} of 276 nm. The results of CIP removal are shown in Figure 5(a). All samples were placed in the dark for 60 min before the visible light irradiation for the adsorption-desorption equilibrium. The removal of CIP without the presence of nanoparticles is due to photolysis (Wang et al. 2021). In the presence of TiO_2, the removal of CIP by TiO_2 was the lowest at about 65%. The highest removal of CIP was achieved at about 91% by 50-Ag/TiO_2, followed by 80-Ag/TiO_2 (88%), 30-Ag/TiO_2 (87%), and 10-Ag/TiO_2 (84%). Notably, the adsorption of CIP on TiO_2 was low compared to the other nanoparticles in the dark region.

The active species involved in the removal of CIP by Ag/TiO_2 were identified through *in situ* trapping experiments. Benzoquinone (BQ), ammonium oxalate (OA), and isopropyl alcohol (IPA) were employed as the scavengers of $\bullet O_2^-$, h^+, and •OH, respectively (Krishnamoorthy et al. 2022). The result of the trapping experiment is presented in Figure 5(b). CIP exhibited the maximum removal efficiency in the absence of scavengers. There was a noticeable decrease in CIP removal to 26% after the addition of BQ, indicating that $\bullet O_2^-$ plays a vital role in the photocatalytic activity of Ag/TiO_2. The decrease in CIP removal to 70% and 69% was observed as OA and IPA were added, suggesting the participation of these reactive species. These results confirm that electron transfer from TiO_2 to Ag facilitates O_2 reduction to $\bullet O_2^-$ at the Ag/TiO_2 interface, while •OH and h^+ play supportive roles in the photocatalytic process.

The recyclability test of 50-Ag/TiO_2 is presented in Figure 5(c). It was demonstrated that the removal efficiency gradually declined with the reaction cycle. The Ag/TiO_2 retained a substantial portion of its photocatalytic activity after repeated cycles, although a gradual decrease in removal efficiency was observed. This decline may be attributed to the partial blockage of active sites by reaction intermediates or degradation byproducts causing slight catalyst deactivation during repeated use (Shi et al. 2023).

A schematic illustration of the proposed mechanism is shown in Figure 6. Upon visible light irradiation,

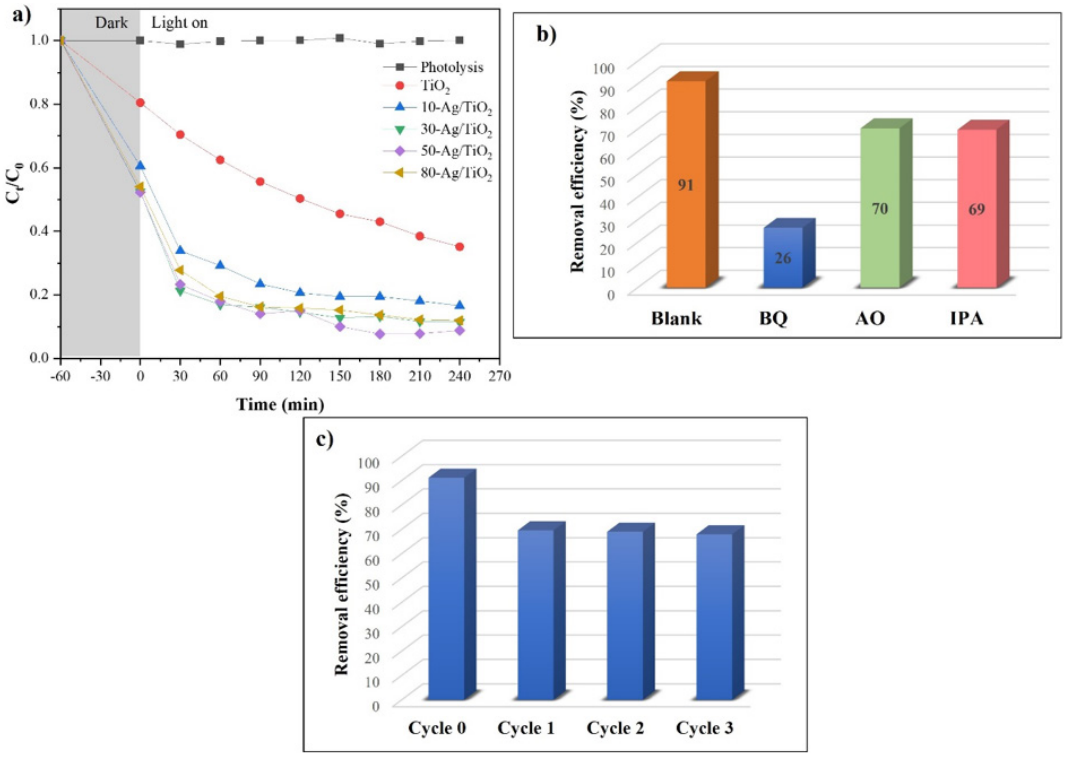


FIGURE 5. a) The photodegradation of CIP using various photocatalysts, (b) the effect of different radical scavengers on the photodegradation of CIP by Ag/TiO_2, and (c) recyclability of 50-Ag/TiO_2

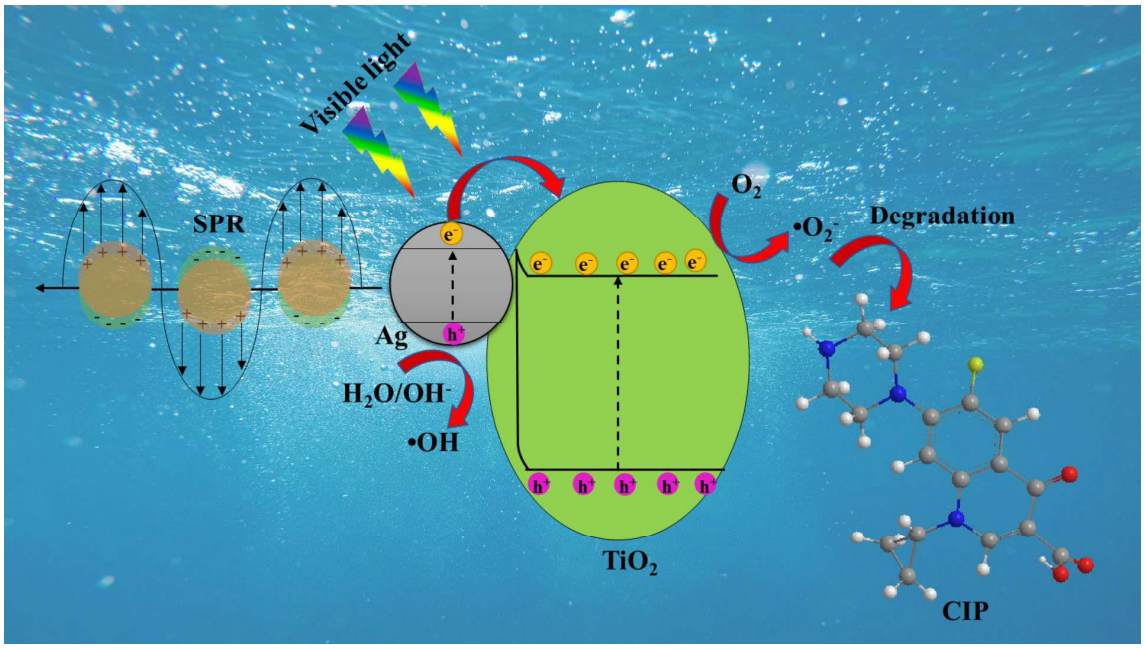


FIGURE 6. Illustration of the degradation mechanism of CIP by Ag/TiO_2

the deposition of Ag on the surface of TiO_2 introduces localized SPR (Kumar et al. 2022; Manuel & Shankar 2021; Michalska et al. 2022). The collective oscillation of conduction electrons in Ag generates energetic and holes pair. These photogenerated electrons on the Ag surface possess sufficient energy to overcome the Schottky barrier formed at the Ag/TiO_2 interface and migrated to the conduction bands of TiO_2 (Zhang et al. 2025). The Ag acts as an electron trap, suppressing electron-hole recombination and promoting charge separation (Yu et al. 2020). Once separated, the photogenerated charge carriers participate in interfacial redox reactions. Electrons transferred into the conduction band of TiO_2 react with dissolved oxygen molecules, leading to the generation of superoxide radicals ($•O_2^-$)(Tahir et al. 2016). The formation of $•O_2^-$ participates in oxidation and thereby facilitates the degradation of CIP. Meanwhile, photogenerated holes (h^+) on the surface of the Ag not only directly oxidize pollutants but also oxidize water to produce hydroxyl radicals (•OH), which also contribute to the degradation process (Abbas, Rasuli & Nakhostin Panahi 2025). Therefore, the combination of SPR effect, efficient charge, and the generation of reactive oxygen species synergistically enhances the visible-light photocatalytic degradation of CIP.

CONCLUSION

In summary, Ag/TiO_2 photocatalysts were successfully synthesized via a one-pot biosynthesis method using OI extract as both a reducing and capping agent due to the presence of phytochemicals, particularly flavonoids. The morphological analyses confirmed the formation of Ag on the surface of anatase TiO_2 and showed the formation of quasi-spherical-shaped nanoparticles. Under visible light irradiation, 50-Ag/TiO_2 showed improved photocatalytic activity towards the removal of CIP by up to 91% compared to pristine TiO_2. Ag-decorated TiO_2 through surface plasmon resonance (SPR) effect and efficient charge separation. The photocatalyst also demonstrated good stability and reusability over repeated cycles. Overall, this work highlights the influence of biosynthesized Ag decoration on the optical response and photocatalytic behaviour of Ag/TiO_2 under visible light irradiation. The combined experimental findings contribute to a clearer understanding of plasmon-enhanced photocatalytic activity in metal-decorated TiO_2 and provide a basis for designing visible-light photocatalysts.

ACKNOWLEDGEMENTS

We gratefully acknowledge the Ministry of Higher Education (MOHE) for the Fundamental Research Grant Scheme under the grant number FRGS/1/2021/STG05/UKM/02/3 and the Faculty of Science and Technology, Universiti Kebangsaan Malaysia (UKM) for providing the research facilities. Thank you to Universiti Teknologi MARA (UiTM) for granting education sponsorship to the first author.

REFERENCES

Abbas, N.H., Rasuli, R. & Nakhostin Panahi, P. 2025. Decorated titanium oxide with Ag nanoparticles as an efficient photocatalyst under visible light: A novel synthesis approach. *Scientific Reports* 15: 8207.

Ahmed Sharwani, A., Badri Narayanan, K., Ehtisham Khan, M. & Soo Han, S. 2021. Sustainable fabrication of silver-titania nanocomposites using goji berry (*Lycium barbarum* L.) fruit extract and their photocatalytic and antibacterial applications. *Arabian Journal of Chemistry* 14(12): 103456.

Alkan, G., Rudolf, R., Bogovic, J., Jenko, D. & Friedrich, B. 2017. Structure and formation model of Ag/TiO_2 and Au/TiO_2 nanoparticles synthesized through ultrasonic spray pyrolysis. *Metals* 7(10): 389.

Amarjargal, A., Tijing, L.D. & Kim, C.S. 2012. Effect of annealing on the phase transition and morphology of Ag NPs on/in TiO_2 rods synthesized by a polyol method. *Ceramics International* 38(8): 6365-6375.

Amutha, E., Sivakavinesan, M., Rajaduraipandian, S. & Annadurai, G. 2023. Identification of phytochemicals capping the biosynthesized silver nanoparticles by *Wrightia tinctoria* and evaluation of their *in vitro* antioxidant, antibacterial, antilarvicidal, and catalytic activities. *Emergent Materials* 6(2): 525-534.

Aslam, M., Abdullah, A.Z. & Rafatullah, M. 2021. Recent development in the green synthesis of titanium dioxide nanoparticles using plant-based biomolecules for environmental and antimicrobial applications. *Journal of Industrial and Engineering Chemistry* 98: 1-16.

Azami, M.S., Nawawi, W.I., Jawad, A.H., Ishak, M.A.M. & Ismail, K. 2017. N-doped TiO_2 synthesised via microwave induced photocatalytic on RR4 dye removal under LED light irradiation. *Sains Malaysiana* 46(8): 1309-1316.

Bhardwaj, D. & Singh, R. 2021. Green biomimetic synthesis of $Ag\text{-}TiO_2$ nanocomposite using *Origanum majorana* leaf extract under sonication and their biological activities. *Bioresources and Bioprocessing* 8: 1.

Cantarella, M., Mangano, M., Zimbone, M., Sfuncia, G., Nicotra, G., Maria Scalisi, E., Violetta Brundo, M., Lucia Pellegrino, A., Giuffrida, F., Privitera, V. & Impellizzeri, G. 2023. Green synthesis of photocatalytic TiO_2/Ag nanoparticles for an efficient water remediation. *Journal of Photochemistry and Photobiology A: Chemistry* 443: 114838.

Chandra, S., Khan, S., Avula, B., Lata, H., Yang, M.H., ElSohly, M.A. & Khan, I.A. 2014. Assessment of total phenolic and flavonoid content, antioxidant properties, and yield of aeroponically and conventionally grown leafy vegetables and fruit crops: A comparative study. *Evidence-Based Complementary and Alternative Medicine* 2014: 253875.

Chelli, V.R., Chakraborty, S. & Golder, A.K. 2018. Ag-doping on TiO_2 using plant-based glycosidic compounds for high photonic efficiency degradative oxidation under visible light. *Journal of Molecular Liquids* 271: 380-388.

Cosmas Mojulat, M.B. & Surugau, N. 2018. Effect of extraction conditions of *Carica papaya* leaves aqueous extracts and its resulting infusion with "kelulut" honey to its antioxidant activity. *ASM Sc. J.* 11(Sp. Issue 2): 75-86.

Davari, N., Falletta, E., Bianchi, C.L., Yargeau, V., Rodriguez-Seco, C. & Boffito, D.C. 2025. Comparing the photocatalytic activity of suspended and floating Ag-decorated TiO_2 for dye removal. *Tetrahedron Green Chem.* 5: 100059.

Gao, B., Wang, J., Dou, M., Xu, C. & Huang, X. 2019. Enhanced photocatalytic removal of amoxicillin with Ag/TiO_2/mesoporous g-C3N4 under visible light: Property and mechanistic studies. *Environmental Science and Pollution Research* 27(7): 7025-7039.

Habibi, M.H. & Nasr-Esfahani, M. 2008. Silver doped TiO_2 nanostructure composite photocatalyst film synthesized by sol-gel spin and dip coating technique on glass. *International Journal of Photoenergy* 2008: 628713.

Hariharan, D., Thangamuniyandi, P., Jegatha Christy, A., Vasantharaja, R., Selvakumar, P., Sagadevan, S., Pugazhendhi, A. & Nehru, L.C. 2020. Enhanced photocatalysis and anticancer activity of green hydrothermal synthesized $Ag@TiO_2$ nanoparticles. *Journal of Photochemistry and Photobiology B: Biology* 202: 111636.

Jagetia, G.C. 2021. A review on the medicinal and pharmacological properties of traditional ethnomedicinal plant Sonapatha, *Oroxylum indicum*. *Sinusitis* 5(1): 71-89.

Jasrotia, T., Chaudhary, S., Kaushik, A., Kumar, R. & Chaudhary, G.R. 2020. Green chemistry-assisted synthesis of biocompatible Ag, Cu, and Fe_2O_3 nanoparticles. *Materials Today Chemistry* 15: 100214.

Jayapriya, M. & Arulmozhi, M. 2021. *Beta vulgaris* peel extract mediated synthesis of Ag/TiO_2 nanocomposite: Characterization, evaluation of antibacterial and catalytic degradation of textile dyes-an electron relay effect. *Inorganic Chemistry Communications* 128: 108529.

Kanakaraju, D., anak Kutiang, F.D., Lim, Y.C. & Goh, P.S. 2022. Recent progress of Ag/TiO_2 photocatalyst for wastewater treatment: Doping, co-doping, and green materials functionalization. *Applied Materials Today* 27: 101500.

Karim, N.A., Rubinsin, N.J., Burukan, M.A.A. & Kamarudin, S.K. 2019. Sustainable route of synthesis platinum nanoparticles using orange peel extract. *International Journal of Green Energy* 16(15): 1518-1526.

Kaur Aulakh, M., Sharma, R., Pal, B. & Prakash, R. 2020. Photo-induced oxidation and reduction by plasmonic $Ag\text{-}TiO_2$ nanocomposites under UV/sunlight. *Solar Energy* 196: 427-436.

Khan, H. & Shah, M.U.H. 2023. Modification strategies of TiO_2 based photocatalysts for enhanced visible light activity and energy storage ability: A review. *Journal of Environmental Chemical Engineering* 11(6): 111532.

Krishnamoorthy, M., Mohamed, M.A., Kaus, N.H.M. & Yusoff, S.F.M. 2022. Adsorption and photocatalytic degradation of cationic dyes over bismuth ferrite (BFO) intercalated on liquid natural rubber-based hydrogel compound. *Journal of Industrial and Engineering Chemistry* 116: 447-464.

Kulal, D. & Shetty Kodialbail, V. 2021. Visible light mediated photocatalytic dye degradation using Ag_2O/AgO-TiO_2 nanocomposite synthesized by extracellular bacterial mediated synthesis - An eco-friendly approach for pollution abatement. *Journal of Environmental Chemical Engineering* 9(4): 105389.

Kumar, A., Choudhary, P., Kumar, A., Camargo, P.H.C. & Krishnan, V. 2022. Recent advances in plasmonic photocatalysis based on TiO_2 and noble metal nanoparticles for energy conversion, environmental remediation, and organic synthesis. *Small* 18(1): 2101638.

Laouini, S.E., Bouafia, A., Soldatov, A.V., Algarni, H., Tedjani, M.L., Ali, G.A.M. & Barhoum, A. 2021. Green synthesized of Ag/Ag_2O nanoparticles using aqueous leaves extracts of *Phoenix dactylifera* L. and their azo dye photodegradation. *Membranes* 11(7): 468.

Lee, J.E., Bera, S., Choi, Y.S. & Lee, W.I. 2017. Size-dependent plasmonic effects of M and M@SiO_2 (M = Au or Ag) deposited on TiO_2 in photocatalytic oxidation reactions. *Applied Catalysis B: Environmental* 214: 15-22.

Li, J., Liu, F. & Li, Y. 2018. Fabrication of an Ag/Ag_2MoO_4 plasmonic photocatalyst with enhanced photocatalytic performance for the degradation of ciprofloxacin. *New Journal of Chemistry* 42(14): 12054-12061.

Manuel, A.P. & Shankar, K. 2021. Hot electrons in TiO_2-noble metal nano-heterojunctions: Fundamental science and applications in photocatalysis. *Nanomaterials* 11(5): 1249.

Mezni, A. 2020. Ternary hybrid Au@Pt-TiO_2 nanocomposites: Highly thermally stable photocatalyst with highly efficient visible-light photocatalytic activity. *Journal of Materials Research and Technology* 9(6): 15263-15272.

Michalska, M., Pavlovský, J., Lemański, K., Małecka, M., Ptak, M., Novák, V., Kormunda, M. & Matějka, V. 2022. The effect of surface modification with Ag nanoparticles on 21 nm TiO_2: Anatase/rutile material for application in photocatalysis. *Materials Today Chemistry* 26: 101123.

Moghni, N., Khalaf, H., Menseri, O., Boutoumi, H., Boudali, R., Dif, F. & Boucheffa, Y. 2025. One–pot green synthesis of TiO_2 nanoparticles using *Inula Viscosa* leaf extract as an efficient photocatalyst for organic dyes removal. *Journal of Photochemistry and Photobiology A: Chemistry* 461: 116158.

Nagaraj, K., Thankamuniyandi, P., Kamalesu, S., Lokhandwala, S., Parekh, N.M., Sakthinathan, S., Chiu, T.W. & Karuppiah, C. 2023. Green synthesis, characterization and efficient photocatalytic study of hydrothermal-assisted Ag@TiO_2 nanocomposites. *Inorganic Chemistry Communications* 148: 110362.

Nasrollahzadeh, M. & Mohammad Sajadi, S. 2016. Green synthesis, characterization and catalytic activity of the Pd/TiO_2 nanoparticles for the ligand-free Suzuki-Miyaura coupling reaction. *Journal of Colloid and Interface Science* 465: 121-127.

Nguyen, V.T. 2020. Sunlight-driven synthesis of silver nanoparticles using pomelo peel extract and antibacterial testing. *Journal of Chemistry* 2020: 6407081.

Paramesh, C.C., Halligudra, G., Muniyappa, M., Shetty, M., Somashekharappa, K.K., Rangappa, D., Rangappa, K.S. & Shivaramu, P.D. 2021. Silver nanoparticles anchored TiO_2 nanotubes prepared using saponin extract as heterogeneous and recyclable catalysts for reduction of dyes. *Ceramics International* 47(10): 14750-14759.

Raduwan, N.F., Shaari, N., Kamarudin, S.K., Masdar, M.S. & Yunus, R.M. 2022. An overview of nanomaterials in fuel cells: Synthesis method and application. *International Journal of Hydrogen Energy* 47(42): 18468-18495.

Rahmawati, T., Butburee, T., Sangkhun, W., Wutikhun, T., Padchasri, J., Kidkhunthod, P., Phromma, S., Eksangsri, T., Kangwansupamonkon, W., Leeladee, P. & Sapcharoenkun, C. 2023. Green synthesis of Ag-TiO_2 nanoparticles using turmeric extract and its enhanced photocatalytic activity under visible light. *Colloids and Surfaces A: Physicochemical and Engineering Aspects* 665: 131206.

Rajangam, K., Amuthameena, S., Thangavel, S., Sanjanadevi, V.S. & Balraj, B. 2020. Synthesis and characterisation of Ag incorporated TiO_2 nanomaterials for supercapacitor applications. *Journal of Molecular Structure* 1219: 128661.

Rao, T.N., Riyazuddin, Babji, P., Ahmad, N., Khan, R.A., Hassan, I., Shahzad, S.A. & Husain, F.M. 2019. Green synthesis and structural classification of *Acacia nilotica* mediated-silver doped titanium oxide (Ag/TiO_2) spherical nanoparticles: Assessment of its antimicrobial and anticancer activity. *Saudi Journal of Biological Sciences* 26(7): 1385-1391.

Rathi, V.H., Jeice, A.R. & Jayakumar, K. 2023. Green synthesis of Ag/CuO and Ag/TiO_2 nanoparticles for enhanced photocatalytic dye degradation, antibacterial, and antifungal properties. *Applied Surface Science Advances* 18: 100476.

Ratshiedana, R., Malefane, M.E., Fakayode, O.J., More, G.K., Mishra, A.K. & Kuvarega, A.T. 2024. Ag induced plasmonic TiO_2 for photocatalytic degradation of pharmaceutical under visible light: Insights into mechanism, antimicrobial and cytotoxicity studies. *Materials Today Communications* 41: 110753.

Rohani, R., Dzulkharnien, N.S.F., Harun, N.H. & Ilias, I.A. 2022. Green approaches, potentials, and applications of zinc oxide nanoparticles in surface coatings and films. *Bioinorganic Chemistry and Applications* 2022: 3077747.

Rojsanga, P., Bunsupa, S. & Sithisarn, P. 2020. Flavones contents in extracts from *Oroxylum indicum* seeds and plant tissue cultures. *Molecules* 25(7): 1545.

Rostas, A.M., Suciu, R.C., Roşu, M.C., Turza, A., Cosma, D.V., Tripon, S., Fort, C.I., Danciu, V., Baia, M., Bocirnea, A. & Indrea, E. 2025. Annealing temperature, a key factor in shaping Ag-decorated TiO_2 aerogels as efficient visible-light photocatalysts. *Materials Chemistry and Physics* 337: 130557.

Sabir, A., Sherazi, T.A. & Xu, Q. 2021. Porous polymer supported Ag-TiO_2 as green photocatalyst for degradation of methyl orange. *Surfaces and Interfaces* 26: 101318.

Saha, B., Kumar, S. & Sengupta, S. 2019. Green synthesis of nano silver on TiO_2 catalyst for application in oxidation of thiophene. *Chemical Engineering Science* 199: 332-341.

Saif, N., Tariq, A., Intisar, A., Batool, Z., Arshad, M., ur Rehman, A. & Kousar, R. 2023. Green synthesis of SnO_2 nanorods and Mo- SnO_2 nanocomposite for efficient sunlight driven organic dye photodegradation in aqueous solution. *Materials Chemistry and Physics* 305: 127920.

Sambaza, S., Maity, A. & Pillay, K. 2019. Enhanced degradation of BPA in water by PANI supported Ag/TiO_2 nanocomposite under UV and visible light. *Journal of Environmental Chemical Engineering* 7(1): 102880.

SatyaEswari, J., Dha-Gat, S., Naik, S., Dibya, S., Swasti, D., Naik, S. & Dibya, S. 2018. Phytochemical and antimicrobial studies of *Oroxylum indicum* extracts. *Pharmaceutical Bioprocessing* 6(1): 7-14.

Selvanathan, V., Shahinuzzaman, M., Selvanathan, S., Sarkar, D.K., Algethami, N., Alkhammash, H.I., Anuar, F.H., Zainuddin, Z., Aminuzzaman, M., Abdullah, H. & Akhtaruzzaman, M. 2021. Phytochemical-assisted green synthesis of nickel oxide nanoparticles for application as electrocatalysts in oxygen evolution reaction. *Catalysts* 11(12): 1523.

Seo, E., Jung, J., Wang, C. & Park, J. 2023. Uniform formation and characterization of Au/TiO_2 nanoparticles for electrokinetically assisted optofluidic reactors. *Micro and Nano Systems Letters* 11: 25.

Shi, Y., Zhang, T., Chang, Q., Ma, C., Yang, Y., Wang, S., Pan, Z., Sun, Y. & Ding, G. 2023. Performance stability and regeneration property of catalytic membranes coupled with advanced oxidation process: A comprehensive review. *Sustainability* 15(9): 7556.

Shi, Y., Huang, J., Zeng, G., Cheng, W. & Hu, J. 2019. Photocatalytic membrane in water purification: Is it stepping closer to be driven by visible light? *Journal of Membrane Science* 584: 364-392.

Singh, J., Kumar, V., Singh Jolly, S., Kim, K.H., Rawat, M., Kukkar, D. & Tsang, Y.F. 2019. Biogenic synthesis of silver nanoparticles and its photocatalytic applications for removal of organic pollutants in water. *Journal of Industrial and Engineering Chemistry* 80: 247-257.

Sun, N., Si, X., He, L., Zhang, J. & Sun, Y. 2024. Strategies for enhancing the photocatalytic activity of semiconductors. *International Journal of Hydrogen Energy* 58: 1249-1265.

Suwannaruang, T., Hildebrand, J.P., Taffa, D.H., Wark, M., Kamonsuangkasem, K., Chirawatkul, P. & Wantala, K. 2020. Visible light-induced degradation of antibiotic ciprofloxacin over Fe-N-TiO_2 mesoporous photocatalyst with anatase/rutile/brookite nanocrystal mixture. *Journal of Photochemistry and Photobiology A: Chemistry* 391: 112371.

Tahir, K., Ahmad, A., Li, B., Nazir, S., Khan, A.U., Nasir, T., Khan, Z.U.H., Naz, R. & Raza, M. 2016. Visible light photo catalytic inactivation of bacteria and photo degradation of methylene blue with Ag/TiO_2 nanocomposite prepared by a novel method. *Journal of Photochemistry and Photobiology B: Biology* 162: 189-198.

Tang, T., Wang, T., Gao, Y., Xiao, H. & Xu, J.H. 2019. Two step method for preparing TiO_2/Ag/rGO heterogeneous anocomposites and its photocatalytic activity under visible light irradiation. *Journal of Materials Science: Materials in Electronics* 30(9): 8471-8478.

Truong, D-H., Nguyen, D.H., Anh Ta, N.T., Bui, A.V., Do, T.H. & Nguyen, H.C. 2019. Evaluation of the use of different solvents for phytochemical constituents, antioxidants, and *in vitro* anti-inflammatory activities of *Severinia buxifolia*. *Journal of Food Quality* 2019: 8178294.

Tseng, H-C. & Chen, Y-W. 2020. Facile synthesis of Ag/TiO_2 by photoreduction method and its degradation activity of methylene blue under UV and visible light irradiation. *Modern Research in Catalysis* 9: 1-19.

Tungmunnithum, D., Thongboonyou, A., Pholboon, A. & Yangsabai, A. 2018. Flavonoids and other phenolic compounds from medicinal plants for pharmaceutical and medical aspects: An overview. *Medicines* 5(3): 93.

Wang, Z., Cai, X., Xie, X., Li, S., Zhang, X. & Wang, Z. 2021. Visible-LED-light-driven photocatalytic degradation of ofloxacin and ciprofloxacin by magnetic biochar modified flower-like Bi_2WO_6: The synergistic effects, mechanism insights and degradation pathways. *Science of The Total Environment* 764: 142879.

Wang, Z., Ali Haidry, A., Xie, L., Zavabeti, A., Li, Z., Yin, W., Lontio Fomekong, R. & Saruhan, B. 2020. Acetone sensing applications of Ag modified TiO_2 porous nanoparticles synthesized via facile hydrothermal method. *Applied Surface Science* 533: 147383.

Yan, M., Wu, Y. & Liu, X. 2021. Photocatalytic nanocomposite membranes for high-efficiency degradation of tetracycline under visible light: An imitated core-shell Au-TiO_2-based design. *Journal of Alloys and Compounds* 855: 157548.

Yildirim, S. 2021. Synthesis, characterization and optical properties of Ag-doped TiO_2 nanoparticles by flame spray pyrolysis. *Journal of Materials Science: Materials in Electronics* 32(12): 16346-16358.

Yin, Y.C., Kait, C.F., Fatimah, H., Wilfred, C., Taha, M.F.B. & Yunus, N.B.M. 2017. Preparation and characterization of Mg/TiO_2 for visible light photooxidative-extractive deep desulfurization. *Sains Malaysiana* 46(3): 493-501.

Yu, Y., Zhu, X., Wang, L., Wu, F., Liu, S., Chang, C. & Luo, X. 2020. A simple strategy to design 3-layered Au-TiO_2 dual nanoparticles immobilized cellulose membranes with enhanced photocatalytic activity. *Carbohydrate Polymers* 231: 115694.

Zarzzeka, C., Goldoni, J., de Paula de Oliveira, J.d.R., Lenzi, G.G., Bagatini, M.D. & Colpini, L.M.S. 2024. Photocatalytic action of Ag/TiO_2 nanoparticles to emerging pollutants degradation: A comprehensive review. *Sustainable Chemistry for the Environment* 8: 100177.

Zhang, S., Li, X., Xie, R., Zhang, X., Wang, H., Song, Y. & Zou, H. 2025. Synergistic introduction of LSPR effect and Schottky junction: Cu@TiO_2 charge regulation achieved efficient, stable photocatalytic removal. *Inorganic Chemistry Frontiers* 12(5): 1979-1993.